Coherent optical interaction between plasmonic nanoparticles and small organic dye molecules in microcavities ©

Cite as: Appl. Phys. Lett. 118, 013301 (2021); https://doi.org/10.1063/5.0027321 Submitted: 28 August 2020 . Accepted: 20 December 2020 . Published Online: 06 January 2021

🧓 K. Mosshammer, M. Sudzius, S. Meister, H. Fröb, A. M. Steiner, 🗓 A. Fery, and 🧓 K. Leo

COLLECTIONS

F This paper was selected as Featured









Your Qubits. Measured.

Meet the next generation of quantum analyzers

- Readout for up to 64 qubits
- Operation at up to 8.5 GHz, mixer-calibration-free
- Signal optimization with minimal latency







Coherent optical interaction between plasmonic nanoparticles and small organic dye molecules in microcavities ••

Cite as: Appl. Phys. Lett. **118**, 013301 (2021); doi: 10.1063/5.0027321 Submitted: 28 August 2020 · Accepted: 20 December 2020 · Published Online: 6 January 2021







K. Mosshammer, ^{1,a)} (D) M. Sudzius, ¹ S. Meister, ¹ H. Fröb, ¹ A. M. Steiner, ² A. Fery, ² (D) and K. Leo ^{1,b)} (D)

AFFILIATIONS

¹Dresden Integrated Center for Applied Physics and Photonic Materials (IAPP) and Institute for Applied Physics, Technische Universität Dresden, 01062 Dresden, Germany

²Leibniz-Institut für Polymerforschung Dresden (IPF), 01069 Dresden, Germany

ABSTRACT

We investigate the lasing performance of different composite gain materials consisting of small organic molecules, gold nanoparticles, and a polymer matrix mixed on a nanoscale within a spin-coated thin film. We experimentally demonstrate that the localized surface plasmon resonances of randomly distributed gold nanoparticles can oscillate in phase with the standing wave of the surrounding microcavity resonator and contribute to a lower lasing threshold.

Published under license by AIP Publishing. https://doi.org/10.1063/5.0027321

The presence of metal films in organic microlaser devices is generally considered detrimental to the lasing action and presents a significant obstacle to the development of electrically driven organic solid state lasers. ^{1–4} This is mostly caused by the absorption of metals, which leads to substantial loss of electromagnetic radiation in the visible range of the spectrum. Approaches to at least partially solve this problem involve the use of carefully designed structures with metal layers incorporated close to the nodes of the standing wave pattern, ^{3–5} periodically structured metallic contacts, ⁶ or cavity-embedded perforated thin metal films. ⁷

On the other hand, light interaction with metals leads to the formation of surface plasmon polaritons on thin-metal-film surfaces⁸ or localized surface plasmon resonances (SPRs) in metallic structures that are small compared to the wavelength. These effects cause the creation of enhanced electric fields near the vicinity of the metal interface, which, in turn, can modify emissive properties of the surrounding optically active materials and, for example, lead to a plasmonenhanced fluorescence. Both radiative and nonradiative decay rates of the excited fluorophore can substantially change when it is coupled to the plasmonic mode. ^{11–13} This interaction between the dipole moment of the molecule and plasmon resonance of the nanoparticle can be very efficient and even lead to the strong coupling effects and corresponding spectral Rabi splitting of the coupled system without any additional optical resonator. ^{14–16}

There exist many convincing demonstrations that these modes can coherently interact with surrounding materials and even lead to lasing on the subwavelength scale. Insertion of metal nanoparticles into the systems exhibiting population inversion of states may lead to cavity-free plasmon-assisted random lasing. In these systems, lasing characteristics are defined by the net effect from the localized surface plasmon resonances of metallic nanoparticles and the scattering efficiency of the random system. Furthermore, periodic arrangements of metal structures incorporated into a conventional microresonator allow for coherent radiation, Section 21,222 and several groups have already demonstrated plasmonic nanolasers with low thresholds.

In this work, we produce thin films that consist of small organic molecules and gold nanoparticles (GoldNP), homogeneously distributed within the polymer matrix. The films are spin-coated on a high-optical quality distributed Bragg reflector (DBR) and have a thickness up to 3 $\lambda/2$ in the vicinity of the sample spinning axis at the emission wavelength of the organic dye. Part of the sample is covered by the top DBR, embedding the organic layer into the cavity. Along with the samples with composite cavity material, we have also prepared a set of similar samples under identical conditions, which do not contain gold nanoparticles (reference samples). The emissive properties of these structures are investigated spectroscopically under soptical pumping by femtosecond pulses.

a) Electronic mail: klara.mosshammer@tu-dresden.de

b) Author to whom correspondence should be addressed: karl.leo@tu-dresden.de

The gold nanoparticles have a trisoctahedral shape [inset of Fig. 1(a)] and were grown via the seed-mediated growth technique. The size and shape of the nanoparticles are precisely controlled by adjusting the kinetics using a syringe pump system during the process. We use gold nanoparticles with their characteristic size of 109 nm. This assures that the SPR occurs in the visible spectral range at 520 nm.

As an emitting material, we choose three different organic dyes: difluoro-3-ethyl-5-[1-(4-ethyl-3,5-dimethyl-2H-pyrrol-2-ylidene-N)ethyl]-2,4-dimethyl-1H-pyrrolato-Nboron (Pyrromethene, PM567), tris-(8-hydroxyquinoline)aluminum (Alq₃), and 4-(dicyanomethylene)-2-methyl-6-(4-dimethylaminostyryl)-4H-pyran (DCM). All of them show a substantial spectral overlap with the extinction coefficient of gold nanoparticles, as shown in Fig. 1.

Mixtures of 1-ethenylpyrrolidin-2-one (Polyvinylpyrrolidone, PVP) polymer matrix, small organic molecules, and gold nanoparticles were prepared at a constant weight ratio of dye 1.0 wt. % to PVP dry mass and PVP equal to 0.03 wt. % to ethanol solvent. For the composite materials, different amounts of gold nanoparticles up to 2.3×10^{10} particles per milliliter have been tested. However, the use of a higher nanoparticle concentration quickly leads to the formation of particle agglomerates, as it is shown in Fig. 2. Particle agglomeration not only

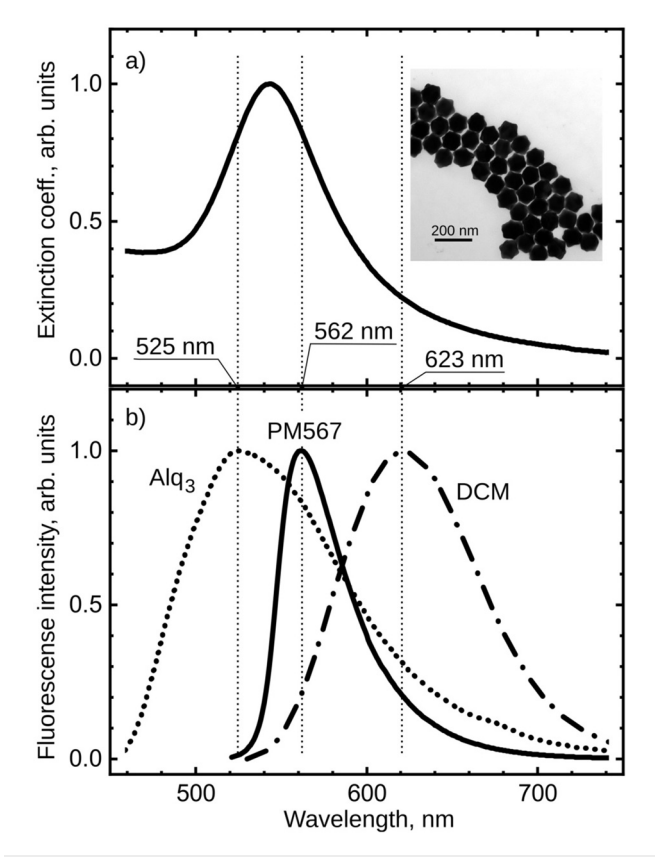


FIG. 1. Extinction coefficient of gold nanoparticles as a function of wavelength (a) and fluorescence spectra of three small molecule organic dyes (b), which have been used to produce composite gain materials. The inset shows the transmission electron microscopy image of a cluster of gold nanoparticles used. The characteristic size of one particle is around 109 nm.

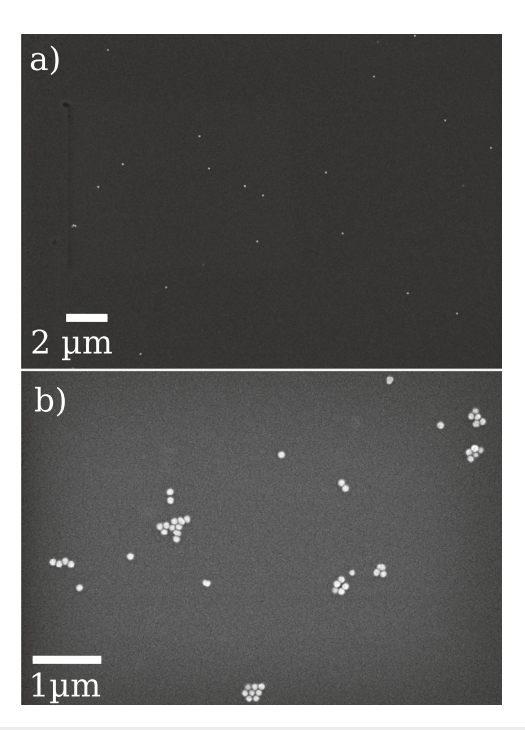


FIG. 2. SEM image of spin-coated PVP layers containing a constant amount of PM567 dye with low (a) and ten times higher (b) concentration of gold nanoparticles.

causes a shift of the SPR resonance frequency but also weakens the interaction between nanoparticles and organic molecules. On the other hand, using a lower particle concentration quickly leads to identical emission spectra from the samples with composite gain materials and the reference samples. Based on these observations, we concentrate further on the empirically found value of 0.7×10^9 particles per milliliter for the composite gain materials; this is the density of the particles, which considerably modifies the emissive properties of the material and still does not cause particle agglomeration.

The samples are prepared on a borosilicate float glass from Schott, which is 1.10 mm thick and possesses an optical flatness better than $\lambda/10$. First of all, the bottom DBR is thermally evaporated under high vacuum conditions. The mirror design wavelength is set close to the organic laser dye fluorescence emission peak. The mirror consists of 21 alternating layers of SiO₂/TiO₂ of $\lambda/4$ optical thickness and has an estimated reflectivity of \sim 99.8% at the design wavelength. As a second step, the composite (or reference) material solution is spin-coated. Although precise control of the thin-film thickness is difficult, it is usually in the range of 3 $\lambda/2$ in the vicinity of the spinning axis at the emission wavelength of the organic dye. Finally, the top DBR, which is identical to the bottom one, is thermally evaporated. During this process, a shadow mask is used to preserve part of the sample to have a top mirror-free area for comparison purposes.

Both PVP/PM567/GoldNP and PVP/DCM/GoldNP cavity-embedded sample regions as well as their corresponding reference samples show lasing under optical pumping by 100 fs pulses at a wavelength of 525 nm. However, we did not observe any difference in emissive properties of PVP/DCM/GoldNP and its reference sample neither

below nor above lasing threshold. We interpret this observation by a rather broad emission spectrum of DCM molecules and its relatively large spectral shift with respect to the extinction function of gold nanoparticles (Fig. 1). In contrast, the spectrum of the PM567 dye is relatively narrow, and its peak intensity is close to the peak value of the extinction coefficient of gold nanoparticles. This causes more effective interaction between PM567 dye molecules and gold nanoparticles than in the DCM case.

The PVP/Alq $_3$ /GoldNP samples did not show lasing when optically pumped at 400 nm in the absorption band of Alq $_3$. Neither of our composite gain materials show any signature of random lasing in top mirror-free areas of the sample. We, therefore, concentrate only on the measurements in the PVP/PM567/GoldNP samples for the rest of this paper.

Figure 3 shows ellipsometry measurements of the refractive index as a function of the wavelength for the spin-coated pure PVP polymer matrix as well as when it is doped with PM567 organic dye or for the composite material with gold nanoparticles added. We estimate the refractive index of \sim 1.53 for composite gain material at the emission wavelength of 560 nm for the PM567 organic dye.

In what follows, we analyze the emissive properties of PVP/ PM567/GoldNP material-based samples below and above lasing threshold at 525 nm femtosecond optical excitation. The signal is collected perpendicular to the sample surface from the small solid angle in order to avoid signal integration over larger angles and to eliminate effects due to microcavity's angular dispersion. The cavity spectra were taken on the sample spots, which show a minimum spectral width of the modes. Figure 4 shows four fluorescence spectra of such a layer from the cavity (C and D) and cavity-free (A and B) regions below lasing threshold. The fluorescence signal is effectively suppressed in the stop band regions of the microresonator (red arrows) and enhanced at the cavity resonance (green arrows). The cavity mode shift is caused by the build-in thickness gradient of the cavity layer due to the spincoating process of the composite gain material. The quality factor Q of the cavity resonance is 103 and 173 for the sample positions C and D, respectively.

We identify lasing from a sharp spectral narrowing of the fluorescence signal above lasing threshold rather than measuring inputoutput curves and precisely identifying lasing thresholds from the

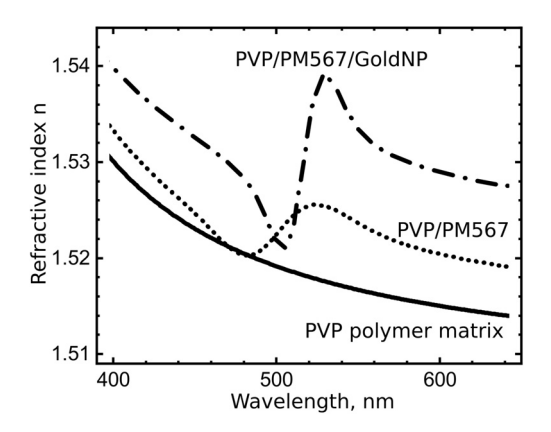


FIG. 3. Variation of the refractive index vs wavelength obtained by ellipsometry for various spincoated PVP polymer matrix-based layers.

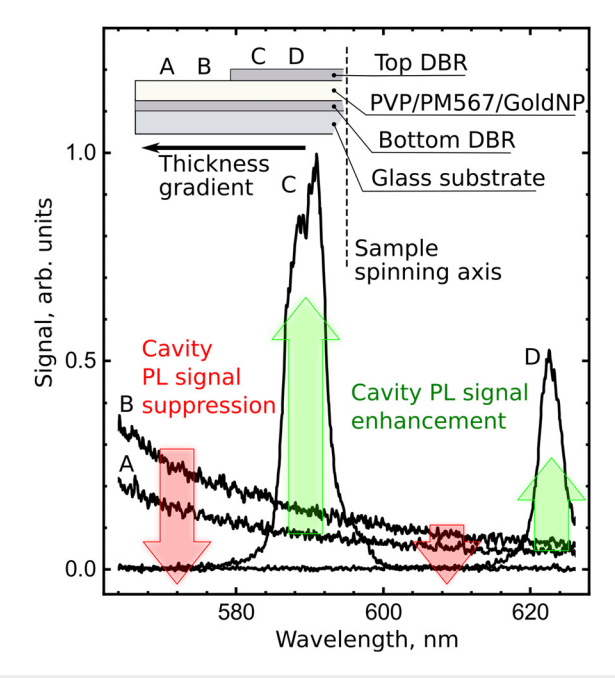


FIG. 4. Fluorescence spectra of the spin-coated PVP/PM567/GoldNP layer thin film measured on four distinct areas of the sample. The structure is schematically shown at the top of the figure. The sample possesses a natural radial wedge due to the spin-coating process. The A and B spectra represent photoluminescence emission from the top mirror-free area, whereas the C and D spectra disclose cavity effects.

exposure characteristics. In this way, we could minimize sample exposure down to a few laser shots of fixed energy and avoid degradation of the PM567 dye in a PVP matrix, which is very pronounced for the femtosecond optical excitation at 525 nm. We repeat every measurement at several different sample positions to collect statistics and minimize possible influences of sample inhomogeneities on the result.

Figure 5 shows emission spectra below and above lasing threshold from organic microcavities based on the PVP/PM567/GoldNP composite gain material.²⁷ The observed spectral narrowing to less than 0.3 nm at higher pump energy is a clear indication of lasing. In the cavities with a composite PVP/PM567/GoldNP gain material, such spectral narrowing was observed in 90% of cases when measured on different places of the sample. In all these cases, the lasing took place in the 570–600 nm spectral range, i.e., close to the peak of the extinction coefficient of gold nanoparticles. Lasing was never observed in the reference sample not containing gold nanoparticles, under the same pumping conditions. Therefore, we consider these observations as clear evidence of a coherent optical interaction between gold nanoparticles and PM567 dye molecules.

The observed reduction of the lasing threshold is a direct consequence of the field enhancement due to the coherent interaction between the microcavity and plasmonic particles. In microcavities with composite gain materials, the cavity field and SPR oscillations coexist. According to Fermi's golden rule, the probability for a small organic molecule to emit spontaneously depends on the electric field it experiences independent of the origin of the field. Although the emission spectra from the cavity-embedded regions in Fig. 4 suggest that

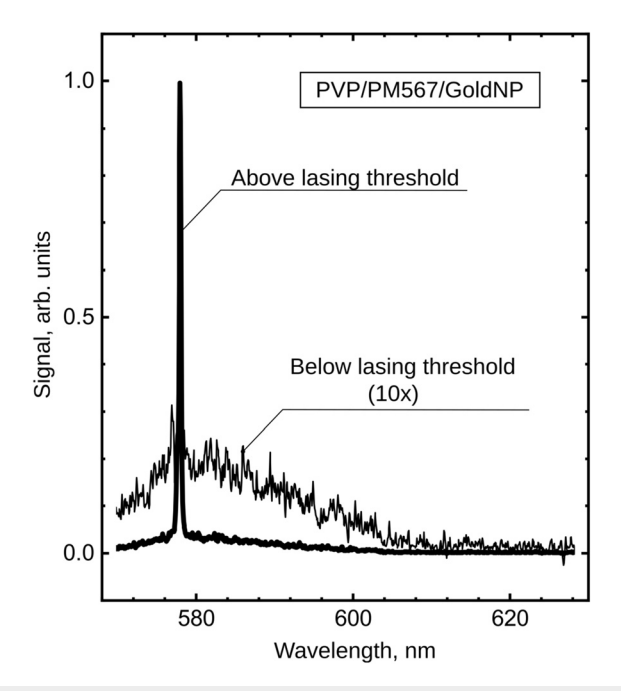


FIG. 5. Emission spectra below and above lasing threshold from the organic microcavity based on PVP/PM567/GoldNP composite gain material.

the cavity field oscillations dominate over the surface plasmon oscillations, the SPR and the cavity fields have to oscillate in phase such that the overall electric field gets enhanced at some point in time. In turn, due to the Purcell effect, the field enhancement leads to a higher emission rate of organic molecules to the mode that will eventually lase. In this way, all three constituents, which possess resonances in the system—planar cavity, plasmonic nanoparticles, and organic molecules—interact with each other in a coherent manner even before the lasing threshold is reached.

In summary, we produced a solid-state organic microcavity laser based on a composite gain material as an optically active layer. The latter consists of PVP as the polymer matrix hosting diluted gold nanoparticles and different organic dyes, which can exhibit population inversion. The resonance of the particles is tuned by shape and size, as well as the DBR design wavelength by layer thicknesses such that they fit the emission spectra of the dye used. We have tested Alq₃, DCM, and PM567 small organic molecule dyes as optically active constituents. Our experimental results indicate that PM567 molecules can effectively couple to the SPR of 109-nm-sized gold nanoparticles. When these molecules are coupled to the cavity field, the SPR oscillations occur in phase with the cavity oscillations in a coherent manner. This coupling leads to the enhancement of the spontaneous emission or lower lasing threshold if the system is operated in a coherent regime.

The authors acknowledge financial support from the DFG through the Würzburg-Dresden Cluster of Excellence on Complexity and Topology in Quantum Matter-ct.qmat (EXC 2147, Project-ID 39085490) and DFG Project Nos. FR 1097/3-1, LE 747/55-1. The assistance of Christian Hänisch in this work is appreciated for helping us to carry out ellipsometry measurements.

DATA AVAILABILITY

The data that support the findings of this study are available from the corresponding author upon reasonable request.

REFERENCES

- ¹M. A. Kaliteevski and A. A. Lazarenko, "Reduced absorption of light by metallic intra-cavity contacts: Tamm plasmon based laser mode engineering," Tech. Phys. Lett. **39**, 698–701 (2013).
- ²M. T. Hill, Y. S. Oei, B. Smalbrugge, Y. Zhu, T. D. Vries, P. J. van Veldhoven, F. W. M. van Otten, T. J. Eijkemans, J. P. Turkiewicz, H. Waardt, E. J. Geluk, S. H. Kwon, Y. H. Lee, R. Nötzel, and M. K. Smit, "Lasing in metallic-coated nanocavities," Nat. Photonics 1, 589–594 (2007).
- ³S. Meister, R. Brückner, M. Sudzius, H. Fröb, and K. Leo, "Optically pumped lasing of an electrically active hybrid OLED-microcavity," Appl. Phys. Lett. 112, 113301 (2018).
- ⁴S. Meister, R. Brückner, M. Sudzius, H. Fröb, and K. Leo, "Intracavity metal contacts for organic microlasers," J. Mater. Res. **34**, 571–578 (2019).
- ⁵R. Brückner, M. Sudzius, S. I. Hintschich, H. Fröb, V. G. Lyssenko, and K. Leo, "Hybrid optical Tamm states in a planar dielectric microcavity," Phys. Rev. B 83, 033405 (2011).
- ⁶R. Brückner, A. A. Zakhidov, R. Scholz, M. Sudzius, S. I. Hintschich, H. Fröb, V. G. Lyssenko, and K. Leo, "Phase-locked coherent modes in a patterned metal-organic microcavity," Nat. Photonics 6, 322–326 (2012).
- ⁷A. Mischok, R. Brückner, M. Sudzius, C. Reinhardt, V. G. Lyssenko, H. Fröb, and K. Leo, "Photonic confinement in laterally structured metal-organic microcavities," Appl. Phys. Lett. 105, 051108 (2014).
- ⁸P. Berini and I. D. Leon, "Surface plasmon-polariton amplifiers and lasers," Nat. Photonics **6**, 16–24 (2012).
- ⁹D. J. Bergman and M. I. Stockman, "Surface plasmon amplification by stimulated emission of radiation: Quantum generation fo coherent surface plasmons in nanosystems," Phys. Rev. Lett. 90, 027402 (2003).
- ¹⁰M. Bauch, K. Toma, M. Toma, Q. Zhang, and J. Dostalek, "Plasmon-enhanced fluorescence biosensors: A review," Plasmonics 9, 781–799 (2014).
- ¹¹S. Kühn, U. Håkanson, L. Rogobete, and V. Sandoghdar, "Enhancement of single-molecule fluorescence using a gold nanoparticle as an optical nanoantenna," Phys. Rev. Lett. 97, 017402 (2006).
- ¹²N. S. Abadeer, M. R. Brennan, W. L. Wilson, and C. J. Murphy, "Distance and plasmon wavelength dependent fluorescence of molecules bound to silicacoated gold nanorods," ACS Nano 8, 8392–8406 (2014).
- ¹³A. V. Akimov, A. Mukherjee, C. L. Yu, D. E. Chang, A. S. Zibrov, P. R. Hemmer, H. Park, and M. D. Lukin, "Generation of single optical plasmons in metallic nanowires coupled to quantum dots," Nature 450, 402–406 (2007).
- 14. Bellessa, C. Bonnand, J. C. Plenet, and J. Mugnier, "Strong coupling between surface plasmons and excitons in an organic semiconductor," Phys. Rev. Lett. 93, 036404 (2004).
- ¹⁵A. Trügler and U. Hohenester, "Strong coupling between a metallic nanoparticle and a single molecule," Phys. Rev. B 77, 115403 (2008).
- 16 M. M. Dvoynenko and J.-K. Wang, "Revisiting strong coupling between a single molecule and surface plasmons," Opt. Lett. 38, 760 (2013).
- ¹⁷T. Zhang and F. Shan, "Development and application of surface plasmon polaritons on optical amplification," J. Nanomater. 2014, 495381.
- ¹⁸Y. Wan and L. Deng, "Recyclable coherent random lasers assisted by plasmonic nanoparticles in DCM-PVA thin films," Opt. Express 27, 27103 (2019).
- ¹⁹K. Cyprych, D. Chateau, A. Désert, S. Parola, and J. Mysliwiec, "Plasmonic nanoparticles driven enhanced light amplification in a local 2D and 3D self-assembly," Nanomaterials 8, 1051 (2018).
- ²⁰O. Popov, A. Zilbershtein, and D. Davidov, "Random lasing from dye-gold nanoparticles in polymer films: Enhanced gain at the surface-plasmon-resonance wavelength," Appl. Phys. Lett. 89, 191116 (2006).
- ²¹N. I. Zheludev, S. L. Prosvirnin, N. Papasimakis, and V. A. Fedotov, "Lasing spaser," Nat. Photonics 2, 351–354 (2008).
- ²²j. Y. Suh, C. H. Kim, W. Zhou, M. D. Huntington, D. T. Co, M. R. Wasielewski, and T. W. Odom, "Plasmonic bowtie nanolaser arrays," Nano Lett. 12, 5769–5774 (2012).

- ²³M. A. Noginov, G. Zhu, A. M. Belgrave, R. Bakker, V. M. Shalaev, E. E. Narimanov, S. Stout, E. Herz, T. Suteewong, and U. Wiesner, "Demonstration of a spaser-based nanolaser," Nature 460, 1110–1112 (2009).
- ²⁴C. Zhang, Y. Lu, Y. Ni, M. Li, L. Mao, C. Liu, D. Zhang, H. Ming, and P. Wang, "Plasmonic lasing of nanocavity embedding in metallic nanoantenna array," Nano Lett. 15, 1382–1387 (2015).
- ²⁵C. Hanske, G. González-Rubio, C. Hamon, P. Formentín, E. Modin, A. Chuvilin, A. Guerrero-Martínez, L. F. Marsal, and L. M. Liz-Marzán, "Large-
- scale plasmonic pyramidal supercrystals via templated self-assembly of monodisperse gold nanospheres," J. Phys. Chem. C **121**, 10899–10906 (2017).
- ²⁶Y. Ma, Q. Kuang, Z. Jiang, Z. Xie, R. Huang, and L. Zheng, "Synthesis of trisoctahedral gold nanocrystals with exposed high-index facets by a facile chemical method," Angew. Chem., Int. Ed. 47, 8901–8904 (2008).
- 27The mode below the lasing threshold appears spectrally broadened due to some cavity thickness variation over the pump beam's spot size.